# 3-Hydroxy-3-methylglutaryl Coenzyme A Reductase Localization in Rat Liver Peroxisomes and Microsomes of Control and Cholestyramine-treated Animals: Quantitative Biochemical and Immunoelectron Microscopical Analyses

Gilbert A. Keller,* Mehran Pazirandeh,‡ and Skaidrite Krisans‡

*Department of Biology, University of California at San Diego, La Jolla, California 92093; and
‡Department of Biology and Molecular Biology Institute, San Diego State University, San Diego, California 92182.
Address reprint requests to Dr. Krisans.

*Abstract.* 3-Hydroxy-3-methylglutaryl coenzyme A (HMG-CoA) reductase, a key regulatory enzyme involved in cholesterol biosynthesis, has recently been reported to be present in rat liver peroxisomes (Keller, G. A., M. C. Barton, D. J. Shapiro, and S. J. Singer, 1985, *Proc. Natl. Acad. Sci. USA*, 82:770–774). Immunoelectron labeling of ultrathin frozen sections of normal liver, using two monoclonal antibodies to purified rat liver microsomal HMG-CoA reductase, indicated that the enzyme is present in the matrix of peroxisomes. This study is a quantitative biochemical and immunoelectron microscopical analysis of HMG-CoA reductase in rat liver peroxisomes and microsomes of normal and cholestyramine-treated animals. Cholestyramine treatment produced a six- to sevenfold increase in the specific activity of peroxisomal HMG-CoA reductase, whereas the microsomal HMG-CoA reductase specific activity increased by about twofold. Using a computer program that calculates optimal linear combinations of marker enzymes, it was determined that between 20 and 30% of the total reductase activity was located in the peroxisomes of cholestyramine-treated animals. Less than 5% of the reductase activity was present in peroxisomes under control conditions. Quantitation of the immunoelectron microscopical data was in excellent agreement with the biochemical results. After cholestyramine treatment there was an eightfold increase in the density of gold particles per peroxisome, and we estimate about a threefold increase in the labeling of the ER.

THE key regulatory enzyme of cholesterol, dolichol, and isopentenyl adenosine biosynthesis, 3-hydroxy-3-methylglutaryl coenzyme A (HMG-CoA)[1] reductase, is a 97-kD transmembrane glycoprotein that was believed until recently to reside exclusively in the endoplasmic reticulum (ER) of mammalian cells (7, 8, 27, 28). However, a recent publication showed that the enzyme in liver cells is present not only in the ER but also within peroxisomes (18). Immunoelectron labeling of ultrathin frozen sections of normal liver, using two monoclonal antibodies to purified rat liver microsomal HMG-CoA reductase, indicated that the enzyme is concentrated in the matrix of peroxisomes.

This study was designed to determine what percentage of the total liver HMG-CoA reductase activity is attributable to the peroxisomal enzyme and to determine if the peroxisomal and the ER enzymes are dependently or independently regulated. Normal rat livers and livers obtained from animals in which the total HMG-CoA reductase activity was increased by cholestyramine treatment were fractionated by differential and density gradient centrifugation.

Two completely independent analyses of the fractions were performed: (*a*) immunoelectron microscopy with quantitation of the antigenic sites of HMG-CoA reductase; and (*b*) quantitative enzyme activity measurements of the subcellular fractions with computer-assisted analyses.

## Materials and Methods

### Animals

Male Sprague-Dawley rats (180–240 g) were used in this study. The animals were acclimatized to a 12-h light–dark cycle for at least 2 wk before each experiment. Standard lab chow was given ad libitum and in some cases supplemented with 5% cholestyramine for 4 d before they were killed. Rats were fasted for 6 h and killed 6 h into their dark cycle by a guillotine.

### Cell Fractionation

Liver homogenates were fractionated into υ, λ, and ψ fractions as described by Leighton et al. (26) except that preinjection of rats with Triton WR-1339 was omitted and the λ fraction was washed only once. The υ fraction contains the nuclei and most of the mitochondria, the λ fraction is enriched in

---

1. *Abbreviations used in this paper*: ER, endoplasmic reticulum; HMG-CoA, 3-hydroxy-3-methylglutaryl coenzyme A.

peroxisomes and lysosomes (similar to the L fraction of deDuve et al. [11]), and the ψ fraction contains the majority of microsomes and soluble components. The λ fraction was then further fractionated by centrifugation on a steep linear metrizamide gradient (20–50%, wt/wt) (4, 16). Routinely, 6 ml of the fraction prepared from six rat livers were loaded on top of a 27-ml linear metrizamide gradient containing a 0.5 ml 50% wt/wt metrizamide cushion. The gradient was centrifuged in a Sorvall OTD 75B centrifuge (DuPont Co., Sorvall Instruments Div., Newton, CT) using a TV 850 ultra-vertical rotor at 40,000 rpm for 60 min at 8°C. A total of 25–30 fractions were collected from the bottom of the centrifuge tube with a two-way needle.

Rat liver microsomes were prepared by separating the ψ fraction into a microsomal and soluble fraction by centrifugation at 100,000 $g$ for 60 min.

## Fixation of Samples for Immunoelectron Microscopy

Small blocks of liver from three control and three cholestyramine-fed animals were chopped in 4% formaldehyde, 0.2% glutaraldehyde in 0.1 M phosphate buffer (pH 7.2), and immersed in the same fixative for 1 h. After washing in 0.1 M phosphate buffer (pH 7.2), the blocks were infused with 2.3 M sucrose and ultrathin sections were obtained as described below.

Samples of the λ fraction (peroxisomal-enriched fraction), the microsomal fraction, and the pure peroxisomal fraction were centrifuged in a Beckman microcentrifuge (Beckman Instruments, Inc., Palo Alto, CA) and washed in 0.2 M phosphate buffer (pH 7.2). The pellet was resuspended in 4% formaldehyde, 0.2% glutaraldehyde in 0.2 M phosphate buffer (pH 7.2). After washing, the pellet was transferred to 10% gelatin in phosphate buffer at 37°C. After solidification at 0°C, the blocks of gelatin-embedded fractions were infused with 2.3 M sucrose, mounted on a copper stub, and frozen in liquid nitrogen.

## Cryoultramicrotomy

Ultrathin frozen sections were cut with a glass knife at −88°C, according to the method of Tokuyasu (38) in a DuPont-Sorvall ultramicrotome MT-2 equipped with the LTC-2 cryoattachment. Ultrathin sections were transferred onto formvar-coated copper grids and immunolabeled.

## Immunolabeling

The characterization of the monoclonal antibody to electrophoretically homogenous HMG-CoA reductase (9) and the immunolabeling procedure used in this study are described elsewhere (19). As reported in this previous paper, the density of immunolabeling in peroxisomes was much higher using the monoclonal antibody A than monoclonal antibody B as the primary reagent (18). Consequently, to obtain maximum immunolabeling density, the monoclonal antibody A was exclusively used for immunolabeling experiments of both rat liver sections and cell fractions. Briefly, for immunolabeling experiments, the primary reagent was the monoclonal antibody A to rat liver ER HMG-CoA reductase used at a concentration of 18 μg/ml, and the secondary reagent was colloidal gold adducts of affinity-purified rabbit antibodies to mouse IgG. Colloidal gold particles of 6–8-nm diam and the adduct were prepared as previously described (19). After immunolabeling, sections mounted on grids were treated with 2% osmium tetroxide, poststained in uranyl acetate, and infused with white acrylic resin (London Resin Co. Ltd., London) (19). After polymerization, the grids were examined without poststaining in a Philips model 300 transmission electron microscope at 80 kV equipped with an 11-μm diam aperture.

## Control Experiments

Liver and cell fraction sections were immunolabeled as described above except that the unrelated control monoclonal antibody JG-9 was used instead of the primary monoclonal to HMG-CoA reductase. A micrograph of liver section immunolabeled with the control antibody was published (18).

## Morphometrical Analysis

Morphometrical analysis was performed essentially as described by Weibel et al. (39). Thin frozen sections (1,000 Å) from three control and three cholestyramine-treated livers were photographed at a magnification of 3,700 and printed at 12,500. Five prints per liver were analyzed and point counting was used to estimate the relative volume of peroxisomes. Morphometrical measurements on the diameter of the organelle were performed on 50 peroxisomes from control rats and 87 peroxisomes from cholestyramine-treated rats.

## Quantitation of Immunolabeling in Peroxisomes

The evaluation was performed on frozen sections of liver from three normal and three cholestyramine-treated animals. 90 micrographs (15 per animal) were taken at a primary magnification of 32,000 and printed at a final magnification of 80,000. The sectional area of each peroxisome was measured using a PAD DT-II A digitizer from Houston Instrument (Austin, TX) connected to an Apple II Plus computer (Apple Computer Inc., Cupertino, CA). The number of gold particles was counted and the density of immunolabeling was calculated by dividing the number of particles by the peroxisomal surface area. 20 micrographs each of thin sections of the λ fraction and of the purified peroxisome fraction from cholestyramine-treated animals were similarly processed.

## Assay of Marker Enzymes

Catalase and cytochrome oxidase activities were measured according to Leighton et al. (26) and Lazarow and de Duve (24), except that a molar absorptivity of 19 mM$^{-1}$ cm$^{-1}$ for cytochrome $c$ was used (40). Esterase was measured according to Beaufay et al. (2). Acid phosphatase was measured according to Bergmeyer et al. (3). Enzyme units are in micromoles per minute except for catalase, which is expressed in the units used by Leighton et al. (26). Protein was determined by the method of Lowry (28a) using bovine serum albumin (BSA) as a standard. Since metrizamide interferes with the determination of protein, aliquots of the gradient samples were first precipitated in 10% TCA.

## Assay of HMG-CoA Reductase

HMG-CoA reductase was measured according to Shapiro et al. (35). Enzyme samples were diluted in 50 mM potassium phosphate buffer, pH 7.4, containing 30 mM EDTA, 200 mM NaCl, and 10 mM dithiothreitol. A range of 20–120 μg of protein was used. The samples were preincubated for 30 min at 37°C before the addition of substrate. Control samples lacking either NADP or enzyme (or enzyme added after termination of the reaction) were routinely included. Only freshly isolated fractions were assayed. Using a microsomal pellet (prepared in 0.25 M sucrose) as a source of HMG-CoA reductase, it was found that high concentrations of metrizamide were inhibitory. To minimize this inhibition, the gradient fractions were assayed in a triple reaction volume, and HMG-CoA reductase activity was corrected for metrizamide inhibition.

## Assay of Cleavage Activity

To rule out the possibility of cleavage enzymes being present and interfering with the HMG-CoA reductase assay by causing substrate depletion and/or inhibition of HMG-CoA reductase activity by cleavage products, the samples were incubated as indicated above under conditions that inactivate the HMG-CoA lyase activity present in fractions containing mitochondria (41), and were chromatographed as described by Young and Berger (42). We did not observe any appreciable cleavage activity or substrate depletion in any of the differential centrifugation fractions, the microsomal fraction, or the peroxisomal samples from the gradient. To confirm that the product produced was mevalonic acid and not a co-migrating cleavage product, the area corresponding to the mevalonic acid region on the thin layer chromatographic plate from microsomal and peroxisomal samples was scraped, eluted, and treated as described by Young et al (43). The profile of the $^3$H-labeled products on thin layer chromatography corresponded closely with that of the $^{14}$C-labeled standard as the lactone, the acid, and the amide.

## Computer Calculations

The distribution of HMG-CoA reductase activity in the various organelle fractions was evaluated quantitatively by a computer program that calculates optimal linear combinations of marker enzymes using a least squares criterion (20).

## Materials

($RS$)-[2-$^{14}$C]-Mevalonolactone and coenzyme A DL-[methyl-$^3$H]-3-hydroxy-3-methylglutaryl were purchased from New England Nuclear (Boston, MA). Other chemicals were from Sigma Chemical Co. (St. Louis, MO). Monoclonal antibodies to rat HMG-CoA reductase were a generous gift from Dr. David Shapiro (University of Illinois, Urbana, IL).

## Results

Blocks of hepatic tissue were prepared for immunoelectron microscopy from the same livers that were subsequently fractionated by differential and density gradient centrifugation. An average of six grids carrying the ultrathin frozen sections of livers from normal and cholestyramine-treated rats and of the different cell fractions were submitted to the same protocol for immunolabeling. Immunolabeling for a particular experiment was carried out on all the sections at the same time and with the same immunoreagents.

### Immunolabeling of Liver Sections

Indirect gold immunolabeling for HMG-CoA reductase in control (A) and cholestyramine-treated animals (B) gave results represented in Fig. 1. In control liver samples, the gold particles were nearly all restricted to the peroxisomes
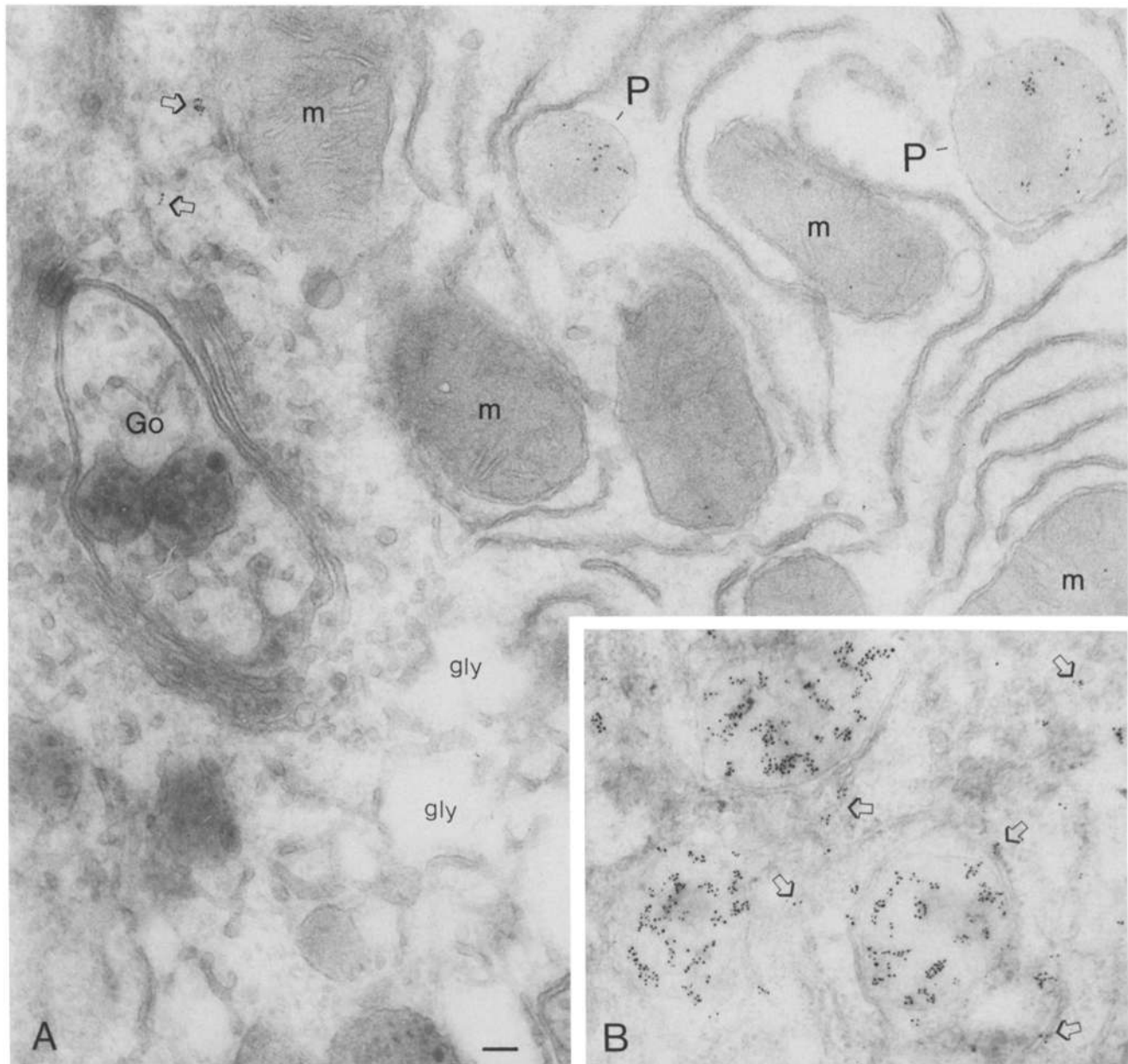


*Figure 1.* Representative micrographs of liver cells from normal (A) and cholestyramine-treated rats (B) that were immunolabeled with a monoclonal antibody against HMG-CoA reductase followed by a colloidal gold adduct of rabbit antibodies to mouse IgG. In the hepatocytes of normal rat (A), gold labels are seen in the matrices of the peroxisomes (P). Clusters of particles (arrows) are only occasionally detected over the elements of the ER. The cisternae of the Golgi apparatus (Go) are free of labeling. The low level of nonspecific labeling can be appreciated by observing the matrices of the mitochondria (m) that are almost totally devoid of gold particles. The peroxisomes from cholestyramine-treated animals (B) contain about eight times as many gold particles as those from normal rats as determined by quantitative evaluation. Furthermore, clusters of gold labels are associated in numerous instances with the cisternae of the ER (arrows). gly, glycogen fields. Bar, 0.1 μm.

(*P*), mostly to the matrix, excluding the crystalloid core. Occasionally, a small number of clustered gold particles were detected in the lamellae of the ER (Fig. 1, arrowhead). The other organelles, in particular the nucleus, the lysosomes, and the cisternae of the Golgi apparatus, showed no labeling. Mitochondria occasionally contained two to four gold particles.

In the liver cells from cholestyramine-treated animals, the pattern of immunolabeling was the same except that the density of gold particles per peroxisome and on the ER cisternae was much higher (*B*). The large increase in immunolabeling density induced by cholestyramine feeding can be appreciated by examination of Fig 1, *A* and *B*. In *B*, the higher enzyme concentration in peroxisomes is obvious. The number of gold particles bound per square micrometer of peroxisome surface from cholestyramine-treated rats and from normal
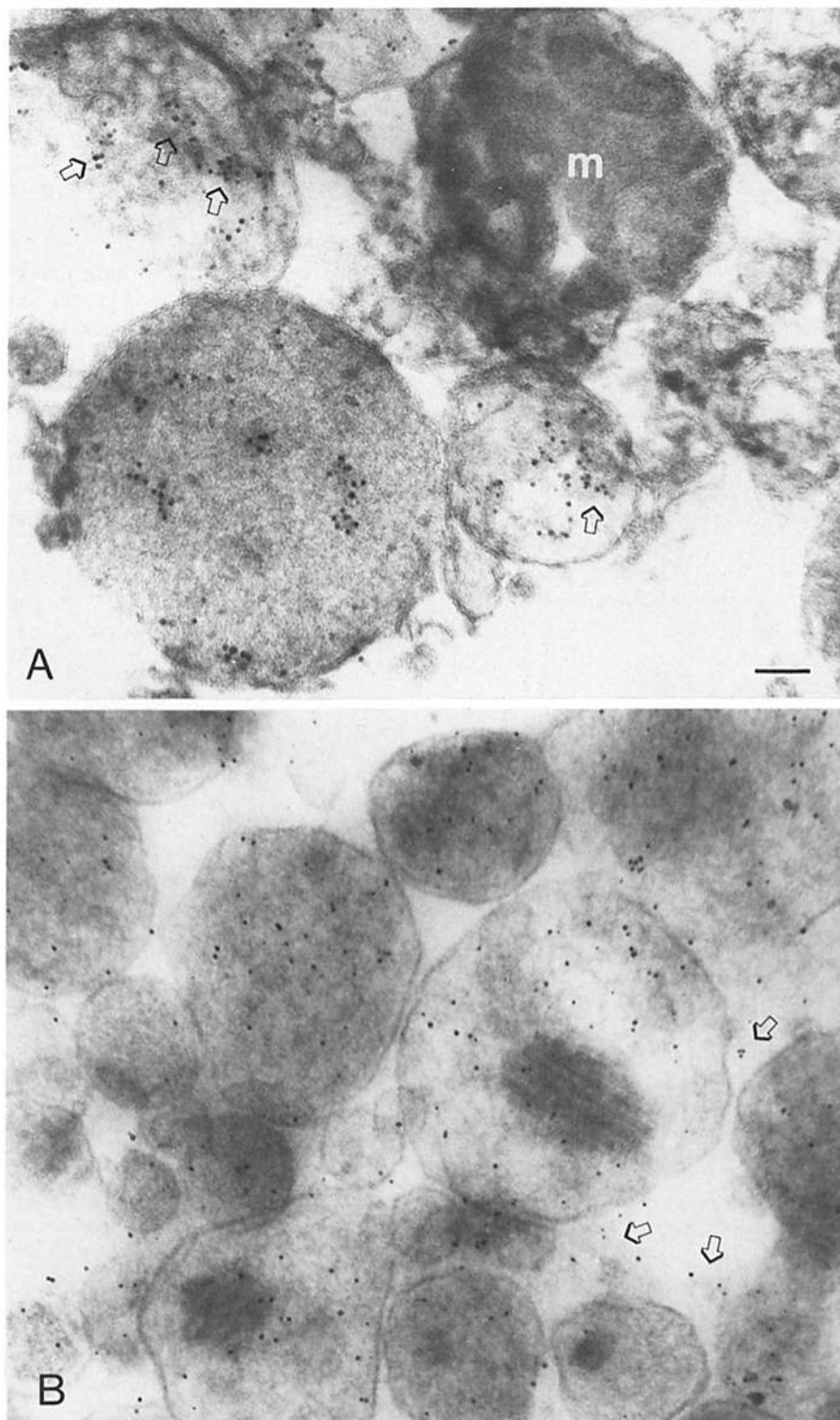


*Figure 2.* Frozen sections of the λ and the pure peroxisome fractions from cholestyramine-treated rats were immunolabeled for the demonstration of HMG-CoA reductase sites. In the λ fraction (*A*), a well-preserved peroxisome contains gold labels. Above and to the right of the peroxisome, vesiculated and elongated elements of presumably endoplasmic origin are also labeled. The swollen mitochondria (*m*) visible in the field is not labeled. The immunolabeling of the pure peroxisome fraction (*B*) shows that almost all peroxisomes contain gold particles even when the matrices appear extracted. The majority of the immunolabeling is visible within the matrix of the organelles. The few gold particles that are not associated with recognizable structures (*arrows*) may be labeling material leaked from damaged peroxisomes or the minor ER contamination. The fine structure of the peroxisomal core is visible in the organelle at the center of the field. The loss of the HMG-CoA reductase molecules during the fractionation procedure is indicated by the decreasing density of the immunolabeling from the intact liver section (Fig. 1 *B*) to the pure peroxisome fraction (Fig. 2 *B*). Bar, 0.1 μm.
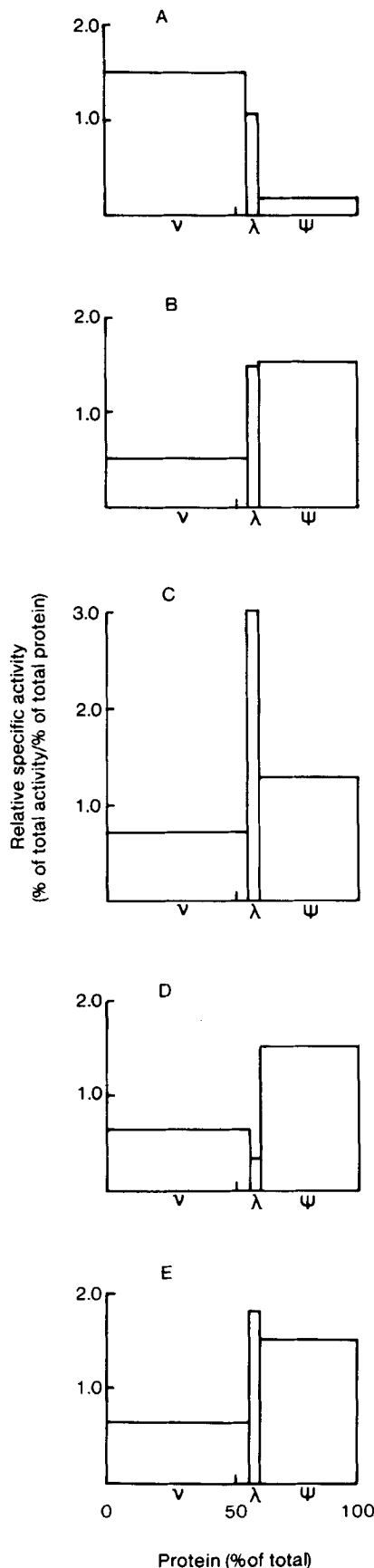
Figure 3. Subcellular distribution of marker enzyme activities and HMG-CoA reductase activity after differential centrifugation of liver extracts from cholestyramine-treated rats. Fractions υ, λ, and ψ are represented from left to right in the order of their isolation and plotted according to de Duve et al. (11). (A) Cytochrome oxidase; (B) esterase; (C) catalase; (D) HMG-CoA reductase; and (E) HMG-CoA reductase treated with acid phosphatase.

rats was 269 ± 9 and 33 ± 4, respectively, indicating that peroxisomes from cholestyramine-fed rats contain about eight times more HMG-CoA reductase molecules than those from normal rats.

Gold labeling was negligible when control monoclonal antibody JG-9 was used.

### Immunolabeling of Cell Fractions

A micrograph of the lambda fraction from a cholestyramine-treated animal that was immunolabeled for HMG-CoA reductase is shown in Fig 2 A. As observed in intact liver sections, the immunolabeling was restricted within the matrix of the organelles. The labeling was also occasionally observed within elongated ER cisternae and vesicles presumably of the same origin. The other recognizable organelles, mitochondria and lysosomes, were devoid of specific labeling. Quantitation of the immunolabeling demonstrated that the peroxisomes in the lambda fraction contained ~50% of the gold particles present in the peroxisomes in situ, 112 ± 13 vs. 269 ± 9 per μm², respectively.

Electron microscopical examination of the pure peroxisomal fraction revealed a nearly homogeneous population of organelles (Fig. 2 B). The peroxisomal membane appeared in most instances intact. The matrix showed a fibrillar or amorphous material after purification as if the organelles had lost their contents during purification. The number of gold particles per peroxisome in the purified fraction was 59 ± 8 per μm², which represents ~20% of the immunolabeling density detected in peroxisomes in situ. Morphometrical measurements showed that the relative volume of peroxisomes remained unchanged after 4 d of cholestyramine treatment; control values were 0.0148 cm³/cm³, as compared with experimental values of 0.0151 cm³/cm³ per hepatocyte cytoplasm. Peroxisomal size also remained unchanged; 0.29 μm ± 0.005 for control vs. 0.30 μm ± 0.006 for experimental.

### Differential Centrifugation

Liver homogenates were first fractionated by differential centrifugation into three fractions, υ, λ and ψ, as described above. All of the fractions were assayed for cytochrome oxidase activity (a mitochondrial marker), catalase activity (a peroxisomal marker), esterase activity (a microsomal marker), and for HMG-CoA reductase activity. Fig. 3 shows the subcellular distribution of the marker enzymes and HMG-CoA reductase activity after differential centrifugation of liver homogenate from cholestyramine-treated rats. Three experiments were performed, each one consisting of livers from six rats. The mean relative specific activities of the enzymes are plotted vs. cumulative protein as described by de Duve et al. (11). Table I gives absolute enzyme activities in whole homogenates, the distribution of these activities in the various fractions, and the recoveries for the experiments illustrated in Fig. 3. The distribution and absolute activities of the marker enzymes after cholestyramine treatment are similar to those of normal rat liver (see Table II), and are in agreement with previous results for normal liver

Table I. *Total Activity and Recovery of Marker Enzymes and HMG-CoA Reductase Activity after Differential Centrifugation of the Homogenates Represented in Fig. 3*

| Enzyme | No. of experiments | Absolute activities*‡ U/g liver (υ + ε)§ | % Distribution | | | Recovery (% of υ + ε) |
|---|---|---|---|---|---|---|
| | | | υ | λ | ψ | |
| Protein | 3 | 216.6 ± 24.1 | 57.4 ± 7.1 | 3.2 ± .97 | 39.3 ± 6.4 | 95.5 ± 8.1 |
| Cytochrome oxidase | 3 | 15.82 ± 3.76 | 88.6 ± 1.6 | 3.5 ± .85 | 7.6 ± 2.3 | 96.8 ± 3.18 |
| Esterase | 3 | 249.0 ± 17.8 | 34.8 ± 13.0 | 4.2 ± 1.5 | 61.0 ± 13.4 | 93.0 ± 8.5 |
| Catalase | 3 | 98.2 ± 7.0 | 39.6 ± 3.0 | 9.8 ± 3.2 | 50.4 ± 2.3 | 95.1 ± 10.3 |
| HMG-CoA reductase | 3 | 205.0 ± 39.0 | 38.1 ± 11.4 | 0.90 ± 0.35 | 60.7 ± 11.0 | 85.6 ± 7.4 |
| HMG-CoA reductase‖ | 1 | 182.7 | 28.8 | 6.3 | 64.9 | 81.0 |

* Calculations are expressed as the mean ± SD.
‡ HMG-CoA reductase activity is expressed in mU/g.
§ ε equals the postnuclear supernatant.
‖ Treated with acid phosphatase.

(15, 26, 29) except that we find more soluble catalase than reported for normal rat liver.

The distribution pattern of HMG-CoA reductase activity illustrated in Fig. 3 D closely coincides with the distribution pattern of esterase, a marker enzyme for ER. These results are in agreement with previous studies (6, 33) and imply that the HMG-CoA reductase activity is located primarily in the ER. However, the activity of HMG-CoA reductase in the λ fraction is less than would be predicted based on the activity of esterase in this fraction.

In normal hepatic tissue ∼15% of the HMG-CoA reductase is present in the active form (dephosphorylated) and 85% exists in the inactive state (phosphorylated) (5). During cell fractionation and subsequent handling of the homogenate, the inactive form of the reductase becomes activated by endogenous phosphatases (34). If phosphatase is primarily in the cytosol, as in rat liver, then reductase sedimenting during the first (low speed) centrifugation will be separated from phosphatase earlier and may be activated less completely than the reductase sedimenting with the microsomes during the high speed centrifugation (42).

To verify that all of the reductase was in the active form after the differential centrifugation of the samples, each fraction was incubated with potato acid phosphatase for 2 h at 37°C as described (31). After the incubation, the HMG-CoA reductase activity was then measured as previously indicated. Fig. 3 E illustrates the results. After acid phosphatase activation (dephosphorylation) the HMG-CoA reductase activity in the λ fraction is clearly increased. The υ and ψ fractions were not significantly affected, indicating the presence of HMG-CoA reductase in its active form in these fractions.

The addition of KF to the λ fraction in conjunction with acid phosphatase abolished the observed increase in HMG-CoA reductase activity. The presence of KF has been shown to prevent in vitro dephosphorylation of HMG-CoA reductase (5). In addition, boiling the acid phosphatase before use also abolished the observed increase. Treatment with acid phosphatase did not change the absolute activity in the whole homogenate. The absolute activity of HMG-CoA reductase in the whole homogenate after cholestyramine treatment is increased over control values (Table I compared with Table II).

## Equilibrium Density Centrifugation

The λ fraction prepared by differential centrifugation from cholestyramine-treated rats was subjected to isopycnic centrifugation in a steep linear metrizamide gradient to separate the organelles on the basis of their different densities. Fig. 4 illustrates one of three typical gradients with recoveries noted. The mitochondria (B) and microsomes (C) are located to the left of the gradient and are responsible for the major peak of protein. The peroxisomes (D) are well separated from the microsomes and mitochondria and are located at greater densities (to the right in Fig. 4). A large portion of the catalase activity is solubilized and sediments at the light end of the gradient. Lysosomes sediment at the far left of the gradient in this system and are well separated from the peroxisomes (data not shown) (16).

The distribution pattern of HMG-CoA reductase activity (Fig. 4 E) shows two peaks, a large peak coincident with microsomes and soluble catalase activity, and a small peak coincident with peroxisomes. These results indicate that

Table II. *Total Activity and Recovery of Marker Enzymes and HMG-CoA Reductase Activity after Differential Centrifugation of Normal Rat Liver Homogenates*

| Enzyme | No. of experiments | Absolute activities*‡ U/g liver (υ + ε)§ | % Distribution | | | Recovery (% of υ + ε) |
|---|---|---|---|---|---|---|
| | | | υ | λ | ψ | |
| Protein | 3 | 230 ± 5.5 | 60.9 ± 2.8 | 3.6 ± 0.5 | 35.4 ± 2.3 | 87 ± 8.0 |
| Cytochrome oxidase | 3 | 15.6 ± 2.4 | 87.7 ± 1.6 | 4.6 ± 0.5 | 6.8 ± 1.7 | 95.5 ± 1.5 |
| Esterase | 3 | 227.5 ± 12.5 | 32.4 ± 6.45 | 5.7 ± 0.2 | 61.9 ± 6.3 | 84.0 ± 11.0 |
| Catalase | 3 | 111.5 ± 2.5 | 40.7 ± 7.0 | 12.3 ± 1.2 | 46.8 ± 5.8 | 96.0 ± 1.0 |
| HMG-CoA reductase | 2 | 89.2 ± 0.8 | 36.0 ± 16.5 | 0.65 ± 0.15 | 63.5 ± 12.1 | 89.5 ± 1.5 |

* Calculations are expressed as the mean ± SD.
‡ HMG-CoA reductase activity is expressed in mU/g.
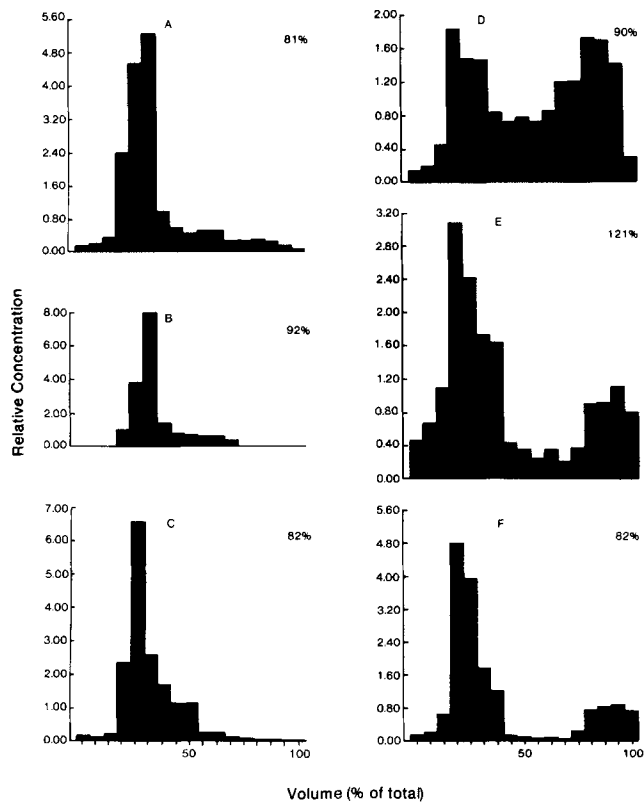§ ε equals the postnuclear supernatant.

880

*Figure 4.* Separation of peroxisomes from other cell organelles. Isopycnic centrifugation in a metrizamide gradient (1.11 g/ml to 1.25 g/ml) of a light mitochondrial (lambda) fraction (see Table I) from cholestyramine-treated animals. The ordinate, relative concentration, is derived by dividing the actual concentration of the enzyme in a particular fraction by the concentration of the enzyme that would be observed if the enzyme would be homogenously distributed throughout the gradient. The abscissa is normalized cumulative volume (the total volume was 32 ml); the area of each graph is thus 1. The density of the gradient increases from left to right. (*A*) Protein; (*B*) cytochrome oxidase; (*C*) esterase; (*D*) catalase; (*E*) HMG-CoA reductase; and (*F*) HMG-CoA reductase treated with acid phosphatase.

part of HMG-CoA reductase activity from cholestyramine-treated rats is located in the peroxisomes. Fig. 4 *F* shows the distribution pattern of HMG-CoA reductase activity after treatment of each gradient fraction with acid phosphatase. The HMG-CoA reductase activity of the purified perox-isomal fractions (dense end of the gradient) was unchanged as a result of acid phosphatase treatment. However, at the light end of the gradient the HMG-CoA reductase activity was increased after incubation with acid phosphatase. This increase in activity was equivalent to that observed in the λ fraction. Again, as in the λ fraction this activation was abolished by the addition of KF or by boiling the acid phosphatase before use.

## Computer Calculations

To interpret the gradient distribution data quantitatively, the amount of HMG-CoA reductase activity in each organelle was determined from the above data by applying the principle of calculating the linear combinations of marker enzyme distributions that would best fit the measured HMG-CoA reductase distributions. This method has been described in
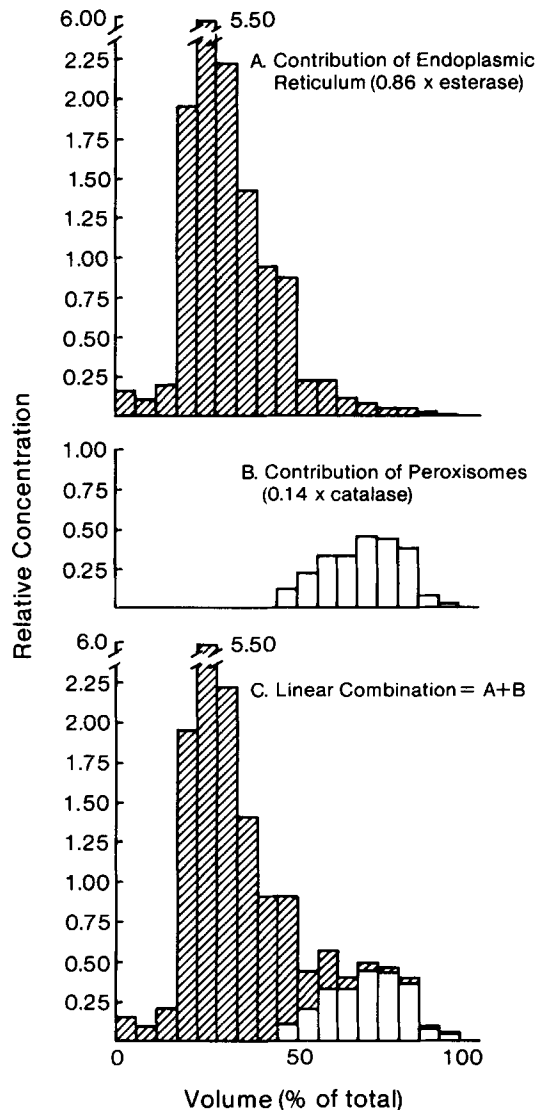


*Figure 5.* Construction of linear combinations for the HMG-CoA reductase distribution of Fig. 4 *F.* The marker enzyme distributions of Fig. 4 are multiplied by the generated coefficients obtained from calculating optimal linear combinations of marker enzymes using a least squares criterion. These calculations were based on the linear combinations of esterase and particulate catalase. Individual contributions of HMG-CoA reductase activity by ER (*A*), peroxisomes (*B*), and the sum of the individual contributions (*C*) are shown.

detail (20). Fig. 5 illustrates the resulting construction of linear combinations for the HMG-CoA reductase activity distribution of Fig. 4 *F.* The results show that 86% of the total activity on the gradient of HMG-CoA reductase is localized in the ER and 14% is localized in the peroxisomes. Correcting for the amounts of the two organelles loaded on the gradient, we calculate that 7% of HMG-CoA reductase activity is localized in the peroxisomes with the remaining 93% in the ER. These calculations were based on the linear combinations of esterase and particulate catalase (i.e., the solubilized catalase activity was deleted). If peroxisomal β-oxidation activity is used as a marker for peroxisomes instead of catalase, the same results are obtained. Peroxisomal β-oxidation activity does not display a soluble com-
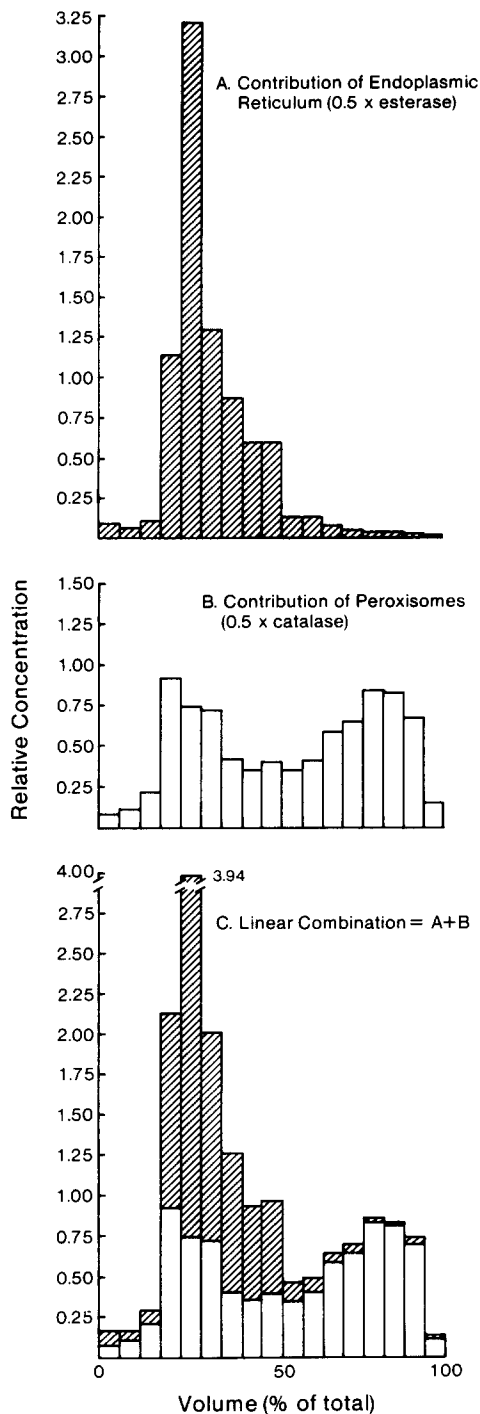
Figure 6. Construction of linear combinations for the HMG-CoA reductase distribution of Fig. 4 F based on the entire catalase distribution. Individual contributions of HMG-CoA reductase activity by ER (A), peroxisomes (B), and the sum of the individual contributions (C) are shown.

ponent (data not shown) (25). However, we cannot rule out the possibility of soluble peroxisomal HMG-CoA reductase activity contributing to some of the HMG-CoA reductase activity in the microsome area. This could be possible since HMG-CoA reductase is located in the matrix of the peroxisomes and could leak out to the soluble portion of the gradient after peroxisome breakage.

Fig. 6 illustrates the construction of linear combinations

for the HMG-CoA reductase activity distribution of Fig. 4 F based on the entire catalase distribution. The results show that 50% of the total activity on the gradient of HMG-CoA reductase is localized in the ER and 50% is now attributed to the peroxisomes. Again, correcting for the amounts of the two organelles loaded on the gradient, we now calculate that 30% of total HMG-CoA reductase activity is localized in the peroxisomes.

To verify if indeed some of the HMG-CoA reductase activity co-migrating with the microsomal fraction on the light end of the gradient was due to solubilized peroxisomal HMG-CoA reductase the following experiment was performed. The fractions from the light end of the gradient (containing the microsomal fraction and solubilized peroxisomal enzymes) were combined and then separated by differential centrifugation into two fractions; a pellet containing the microsomal fraction and a soluble fraction. The samples were treated with acid phosphatase and assayed for HMG-CoA reductase activity. For comparison, pure peroxisomal fractions and microsomal fractions were similarly separated by differential centrifugation into a pellet and soluble fraction. The results are shown in Table III. The results indicate that 40% of the total HMG-CoA reductase activity from the light end of the gradient was in the soluble fraction. This activity clearly is not due to the solubilization of HMG-CoA reductase from microsomes, since <2% of the HMG-CoA reductase activity from the purified microsomal fraction is found in the soluble fraction after similar treatment. However, the amount of HMG-CoA reductase activity solubilized from the peroxisomal fraction (62%) is very similar to that of catalase released (53%). These data indicate that about half of HMG-CoA reductase activity co-migrating with the microsomal fraction on the gradient is due to solubilized HMG-CoA reductase activity released from damaged peroxisomes. Therefore, the linear combination of Fig. 6 based on the entire catalase distribution gives the most accurate calculation of peroxisomal HMG-CoA reductase activity.

Since HMG-CoA reductase in the peroxisomes is located in the matrix, we wanted to confirm that we were measuring all of the HMG-CoA reductase activity of the organelle. Pure peroxisomal samples were assayed for HMG-CoA reductase activity in the presence and absence of varying concentrations of Triton X-100. No difference in activity was observed. This indicates that the peroxisomal enzyme is not latent and that total activity is being measured on the gradient.

Calculations based on the entire catalase distribution, performed on three separate gradients from cholestyramine-treated rats, gave similar values. Based on these results, we conclude that at least 20% but not >30% of total HMG-CoA reductase activity is localized in peroxisomes after cholestyramine treatment.

The HMG-CoA reductase activity distribution obtained after density gradient centrifugation of normal liver had very little activity in the peroxisome area (Fig. 7). We calculate that <5% of total HMG-CoA reductase activity is localized in the peroxisomes under normal conditions. The acid phosphatase studies were not performed on the normal gradient.

## Specific Activity of HMG-CoA Reductase

The specific activity of HMG-CoA reductase was calculated for the most highly purified fractions obtained for each or-

*Table III. Distribution of HMG-CoA Reductase Activity and Marker Enzymes after Differential Centrifugation*

| | Gradient samples* | | | Peroxisomal fraction‡ | | | Microsomal fraction§ | | |
|---|---|---|---|---|---|---|---|---|---|
| | Soluble | Pellet | (Rec.) | Soluble | Pellet | (Rec.) | Soluble | Pellet | (Rec.) |
| | % of total activity | | | | | | | | |
| HMG-CoA reductase | 40 | 60 | 97 | 62 | 38 | 95 | 1.5 | 98.5 | 81 |
| Esterase | 5 | 95 | 98 | – | – | – | 1 | 99 | 106 |
| Catalase | 95 | 5 | 116 | 53 | 47 | 90 | – | – | – |

* Pooled samples from cholestyramine-treated animals after metrizamide density gradient separation, corresponding to the microsomal peak areas and soluble catalase. The combined fractions were centrifuged at 100,000 g for 60 min.
‡ The purity of the peroxisomal fraction, obtained from the dense end of the gradient, is 95%.
§ The purity of the microsomal fraction is 92%. The microsomal fraction was prepared as described in Materials and Methods.

ganelle. The purity of peroxisomes was calculated to be between 92 and 95% based on the measurement of specific marker enzymes (12). The activities of cytochrome oxidase (a mitochondrial marker) and acid phosphatase (a lysosomal marker) in the purified peroxisome fractions were below the level of detection. The major contaminant (5–8%) was the ER. The microsome fraction (prepared by differential centrifugation) was calculated to be 90–95% pure. Table IV shows the specific activities of HMG-CoA reductase measured in purified peroxisomes and microsomes from liver obtained from normal and cholestyramine-treated animals. The peroxisomal HMG-CoA reductase specific activity increases about sevenfold after cholestyramine treatment. However, the microsomal HMG-CoA reductase specific activity increases about twofold, which is consistent with reported literature values (13).

## Discussion

The data from the cell fractionation studies demonstrate that the majority of the HMG-CoA reductase activity is associated with the microsomal fraction both from normal and cholestyramine-treated rats. How can we then explain the low immunolabeling of the ER? The efficiency of immunolabeling on frozen sections depends on the primary fixation which may alter the antigenicity of the protein, on the characteristics of the immunoreagents, and on the conformation of the antigen, and also on the accessibility of immunoreagents to the antigen (32, 36). The HMG-CoA reductase molecules localized in the peroxisomal matrix thus could be more accessible to the immunoreagents, which may explain the higher density of labeling in the peroxisomes, and the impression based on the immunolabeling that in normal liver cells HMG-CoA reductase is exclusively contained in peroxisomes (Fig. 1 A). The monoclonal antibody used was raised against the 55-kD portion of the microsomal HMG-CoA reductase (9); consequently, it recognizes also the portion of the protein that projects into the cytoplasm (9, 27). The few gold particles that can be observed within the lumen of the ER are assumed to have reacted with this cytoplasmic portion of the enzyme. Quantitation of the immunoelectron microscopal data indicated an eightfold increase in the immunolabeling per peroxisome after cholestyramine treatment. And, we estimate about a threefold increase in the immunolabeling of the ER cisternae after cholestyramine treatment.

The biochemical results were in excellent agreement with the quantitative immunoelectron microscopical data. The specific activity of microsomal HMG-CoA reductase in-

creased about twofold after cholestyramine treatment (consistent with literature values [31]), whereas the specific activity of peroxisomal HMG-CoA reductase increased six- to sevenfold. Cholestyramine can cause an increase in ER HMG-CoA reductase activity by several different mechanisms. Clarke et al. (10) reported a fourfold increase in rat liver HMG-CoA reductase mRNA upon cholestyramine treatment. The increase in activity after cholestyramine feeding has also been attributed in part to a threefold activation of the enzyme (37). Finally, cholestyramine treatment could alter the microsomal membrane in regards to cholesterol content and this change can influence the activity of HMG-CoA reductase (30). Whether different mechanisms are involved in the activation of the peroxisomal enzyme is not known at this point. Our results from the immunoelectron study support the observation of Clarke et al. (10), indicating increased enzyme synthesis.

The peroxisomal HMG-CoA reductase specific activity was calculated from the most purified peroxisomal fractions obtained from the metrizamide gradients. We may be underestimating this activity for the following reasons: (a) metrizamide interferes with the measurement of the HMG-CoA reductase activity on the gradient and the correction for metrizamide concentration in the purified peroxisomal fractions was based on measurement of inhibition of microsomal HMG-CoA reductase (prepared in 0.25 M sucrose) and most importantly, (b) the immunoelectron microscopical data indicate a progressive decrease in the density of immunolabeling per peroxisome during purification of these organelles from control and cholestyramine-treated animals. We calculate that peroxisomes in the purified peroxisomal fraction contain only 20% of the gold labeling of peroxisomes in situ. This indicates that the enzyme is soluble within the peroxisomal matrix and, like peroxisomal thiolase and catalase, can be lost due to leakage (1).

Because of the different conditions of organelle preparation and enzyme measurements it may be misleading to directly compare the specific activity of ER HMG-CoA reductase with peroxisomal HMG-CoA reductase. However, the comparison of the relative increase in HMG-CoA reductase activity between control and cholestyramine-treated animals within each organelle is warranted.

In the present study the construction of linear combinations for the HMG-CoA reductase activity distribution after cholestyramine treatment was obtained by two different means: (a) using only particulate catalase or peroxisomal β-oxidation enzymes as markers for peroxisomal HMG-CoA reductase activity and (b) using the entire catalase distri-
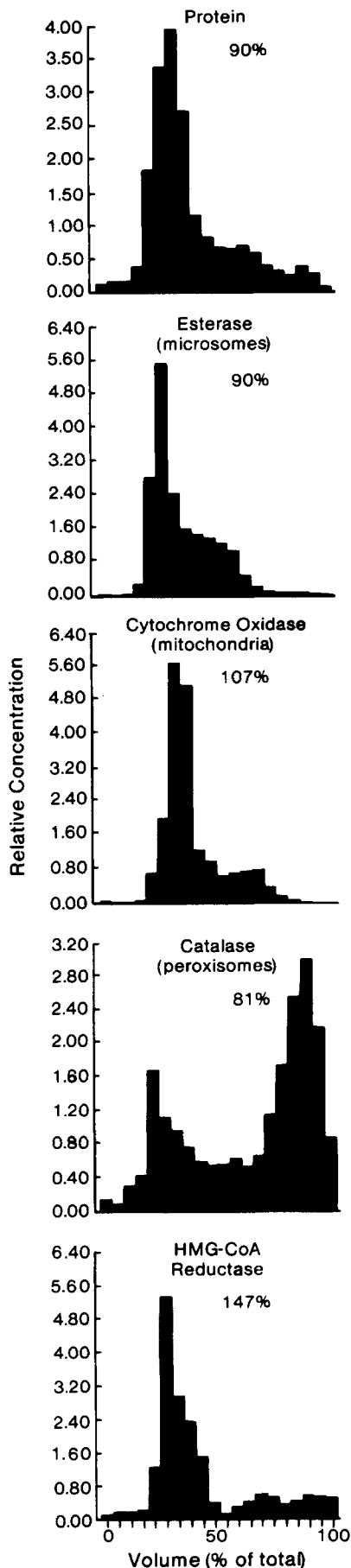
Figure 7. Separation of peroxisomes from other cell organelles. Isopycnic centrifugation in a metrizamide gradient (1.11 g/ml to 1.25 g/ml) of a light mitochondrial (lambda) fraction (see Table II) from normal rat liver. The density of the gradient increases from left to right.

Table IV. Specific Activity of HMG-CoA Reductase*

|  | Normal |  | Cholestyramine |  |
|---|---|---|---|---|
|  | *nmol/min per mg* |  |  |  |
| Peroxisomes | (2)‡ | 0.30 ± 0.18 | (6) | 2.0 ± 0.4 |
| Microsomes | (2) | 2.3 ± 0.1 | (5) | 3.8 ± 1.1 |

* All values given as mean and SD.
‡ The numbers in parentheses refer to number of samples analyzed.

bution (soluble and particulate activity) to determine the percentage of activity of HMG-CoA reductase localized in peroxisomes. We calculate that in drug-treated rats 7% of HMG-CoA reductase is present in peroxisomes based on the particulate catalase distribution and as high as 30% of the enzyme is localized in peroxisomes if the entire catalase distribution is used. We also have shown that part of the HMG-CoA reductase activity on the gradient in the microsome area is a result of soluble peroxisomal HMG-CoA reductase activity (Table III). Thus, the calculations obtained using the entire catalase distribution provide a more accurate percentage and also produce a better fit to the experimental data. Table V shows a summary of the measured and calculated activities of HMG-CoA reductase in rat liver peroxisomes and microsomes from control and cholestyramine-treated animals. The measured values of total HMG-CoA reductase activity in the whole liver compare quite well to the calculated total activity based on specific activity values in both control and cholestyramine groups (first two columns, Table V).

The calculations based on the linear combinations of marker enzymes yield a greater contribution of peroxisomal HMG-CoA reductase activity. Some of this discrepancy in the calculated values may be attributable to the loss of peroxisomal activity during purification. It is interesting to note that if a correction of fivefold is made in the specific activity of peroxisomal HMG-CoA reductase (based on the immunolabeling microscopical data) then the percentage of activity calculated in peroxisomes (last two columns, Table V) would be in excellent agreement.

These calculations were obtained using the HMG-CoA reductase activity distribution after treatment with acid phosphatase. If the nontreated activity distribution is used, the percentage of activity of HMG-CoA reductase localized in peroxisomes increases by 10%. This is due to the activation of the enzyme at the light end of the gradient, resulting in a decrease in relative concentration of activity in the peroxisome area, and a corresponding increase in the microsome and soluble HMG-CoA reductase area (Fig. 4 E compared with Fig. 4 F).

The exact mechanism of this effect is not clear. It appears that a majority of the enzyme in the λ fraction is in the inactive form (phosphorylated) and treatment with acid phosphatase results in dephosphorylation. However, on the gradient, activation is only observed at the light end of the gradient. This implies that the components responsible for phosphory-

*Table V. Measured and Calculated Activity of HMG-CoA Reductase in Rat Liver Peroxisomes and Microsomes from Control and Cholestyramine-treated Animals*

| | nmol/min per g* | nmol/min per g‡ | Percentage of activity in each organelle§ | Percentage of activity in each organelle‖ |
|---|---|---|---|---|
| Control | 88 | 1.9 Peroxisomes<br>115.9 Microsomes<br>117.8 | 1.6 Peroxisomes<br>98.4 Microsomes | 0–5 Peroxisomes<br>95–100 Microsomes |
| Cholestyramine | 205 | 12.5 Peroxisomes<br>190.0 Microsomes<br>202.5 | 6.2 Peroxisomes<br>93.8 Microsomes | 20–30 Peroxisomes<br>70–80 Microsomes |

\* Measured values of HMG-CoA reductase in whole liver (υ + ε fraction from Table I and Table II).
‡ Calculated values of HMG-CoA reductase in whole liver, assuming that there are 6.25 mg of peroxisomal protein and 50 mg of microsomal protein/g of liver, wet weight. Calculations based on HMG-CoA reductase measured per milligram peroxisomal protein or per milligram microsomal protein.
§ Percentage of activity in each organelle, calculated from second column.
‖ Percentage of activity in each organelle, calculated from linear combinations of marker enzymes using the entire catalase distribution. The range is based on calculations from three separate gradients.

lation (for instance HMG-CoA reductase kinase and/or an endogenous pool of ATP and Mg) have been separated on the gradient and do not sediment with the intact peroxisomes.

The biological significance of the localization of the enzyme in two different compartments of the cell remains to be elucidated. There are several conceivable explanations for the presence of the enzyme in peroxisomes as discussed by Keller et al. (18). It appears from this study that the HMG-CoA reductase found in the peroxisomes is not due to the incorporation of a proteolytic fragment of the 97-kD glycoprotein of the ER that is enzymatically active. If it simply were a degradation product, one would expect to see similar increases in enzyme concentration and activity in the two organelles as a result of cholestyramine treatment. Clearly, the data do not show this. Also, we have preliminary data which indicate that peroxisomes contain both a 97-kD polypeptide as well as a 55-kD fragment (21). Thus, there may be two different reductase proteins catalyzing the same reaction in the two organelles. This is the case for other enzymatic "duplications" such as the β-oxidation enzymes (14).

The presence of HMG-CoA reductase in peroxisomes raises intriguing questions about the specific role of these organelles in cellular metabolism. It is now well known that rat liver peroxisomes contain enzymes that catalyze the β-oxidation of fatty acids, a major pathway of lipid metabolism previously thought to operate only in mitochondria (23, 25). Furthermore, it has been demonstrated that the key enzymes of the biosynthetic pathway of glycero-lipids are highly concentrated in liver peroxisomes as well as in microperoxisomes of rat brain (16). In addition, recent results indicate that liver peroxisomes play a role in the biosynthesis of bile acids. Kase et al. (17) found that rat hepatic peroxisomes have the ability to oxidize 3α,7α,12α-trihydroxy-5-β-cholestanoic acid (an intermediate of bile acid synthesis) to cholic acid. Hagey and Krisans (15) reported that the side chain of cholesterol is cleaved by rat peroxisomal fractions. And finally, Krisans et al. (22) showed that highly purified rat liver peroxisomes can oxidize 26-hydroxy-cholesterol to 3-β-hydroxy-5-cholenoic acid (a mono-hydroxy bile acid). These data as well as the present study suggest that peroxisomes may play an important role in regulation of cholesterol metabolism, but the nature of this role is not yet clear.

*References*

1. Alexon, S. E., Y. Fujiki, H. Shio, and P. B. Lazarow. 1985. Partial disassembly of peroxisomes. *J. Cell Biol.* 101:294–304.
2. Beaufay, H., A. Amar-Costesec, E. Feytmans, D. Thines-Sempoux, M. Wibo, M. Robbi, and J. Berthet. 1974. Analytical study of microsomes and isolated subcellular membranes from rat liver. I. Biochemical Methods. *J. Cell Biol.* 61:188–200.
3. Bergmeyer, H. V., K. Gawehn, and M. Grassl. 1974. *In* Methods of Enzymatic Analysis. 2nd English ed. Vol. 1. H. V. Bergmeyer, editor. Verlag-Chemie, Weinheim. Academic Press, Inc., New York. 495–496.
4. Bronfman, M., N. C. Inestrosa, and F. Leighton. 1979. Fatty acid oxidation by human liver peroxisomes. *Biochem. Biophys. Res. Commun.* 88:1030–1036.
5. Brown, M. S., J. L. Goldstein, and J. M. Dietschy. 1979. Improved methods for the assay and activation of 3-hydroxy-3-methyl-glutaryl coenzyme A reductase in the liver of the rat. Comparison with the rate of cholesterol synthesis in different physiological states. *J. Biol. Chem.* 254:5144–5149.
6. Bucher, N. L., P. Overath, and F. Lynen. 1960. B-hydroxy-B-methylglutaryl coenzyme A reductase, cleavage and condensing enzymes in relation to cholesterol formation in rat liver. *Biochim. Biophys. Acta.* 40:491–501.
7. Chin, D. J., K. L. Luskey, J. R. Faust, R. J. MacDonald, M. S. Brown, and J. L. Goldstein. 1982. Molecular cloning of 3-hydroxy-3-methylglutaryl coenzyme A reductase and evidence for regulation of its mRNA. *Proc. Natl. Acad. Sci. USA.* 79:7704–7708.
8. Chin, D. J., G. Gil, D. W. Russell, L. Liscum, K. L. Luskey, S. K. Basu, H. Okayama, P. Berg, J. L. Goldstein, and M. S. Brown. 1984. Nucleotide sequence of 3-hydroxy-3-methylglutaryl coenzyme A reductase, a glycoprotein of endoplasmic reticulum. *Nature (Lond.).* 308:613–617.
9. Clark, R. E., G. G. Martin, M. C. Barton, and D. J. Shapiro. 1982. Production and characterization of monoclonal antibodies to rat liver microsomal 3-hydroxy-3-methylglutaryl-coenzyme A reductase. *Proc. Natl. Acad. Sci. USA.* 79:3734–3738.
10. Clarke, C. F., P. A. Edwards, S. F. Lan, R. D. Tanaka, and A. L. Fogelman. 1983. Regulation of 3-hydroxy-3-methylglutaryl coenzyme A reductase m-RNA levels in rat liver. *Proc. Natl. Acad. Sci. USA.* 80:3305–3308.
11. de Duve, C., B. C. Pressman, R. Gianetto, R. Wattiaux, and F. Appelmans. 1955. Tissue fractionation studies VI. Intracellular distribution patterns of enzymes in rat liver tissue. *Biochem. J.* 60:604–617.
12. Fujiki, Y., S. Fowler, H. Shio, A. L. Hubbard, and P. B. Lazarow. 1982. Polypeptide and phospholipid composition of the membrane of rat liver peroxisomes: comparison with endoplasmic reticulum and mitochondrial membranes. *J. Cell Biol.* 93:103–110.
13. Goldfarb, S., and H. C. Pitot. 1972. Stimulatory effect of dietary lipid and cholestyramine on hepatic HMG-CoA reductase. *J. Lipid Res.* 13:797–801.
14. Hashimoto, T. 1982. Individual peroxisomal β-oxidation enzymes. *Ann.*

*NY Acad. Sci.* 386:5–12.

15. Hagey, L. R., and S. K. Krisans. 1982. Degradation of cholesterol to propionic acid by rat liver peroxisomes. *Biochem. Biophys. Res. Commun.* 107:834–841.

16. Hajra, A. K., and J. F. Bishop. 1982. Glycerolipid biosynthesis in peroxisomes via the acyl dihydroxyacetone phosphate pathway. *Ann. NY Acad. Sci.* 386:170–182.

17. Kase, F., I. Bjorkhem, and J. I. Pederson. 1983. Formation of cholic acid from 3α, 7α, 12α-trihydroxy-5-β-cholestanoic acid by rat liver peroxisomes. *J. Lipid Res.* 24:1560–1567.

18. Keller, G. A., M. C. Barton, D. J. Shapiro, and S. J. Singer. 1985. 3-Hydroxy-3-methylglutaryl coenzyme A reductase is present in peroxisomes in normal rat liver cells. *Proc. Natl. Acad. Sci. USA.* 82:770–774.

19. Keller, G-A., K. T. Tokuyasu, A. H. Dutton, and S. J. Singer. 1984. An improved procedure for immunoelectron microscopy: ultrathin plastic embedding of immunolabeled ultrathin frozen sections. *Proc. Natl. Acad. Sci. USA.* 81:5744–5747.

20. Krisans, S. K., R. M. Mortensen, and P. B. Lazarow. 1980. Acyl-CoA synthetase in rat liver peroxisomes. *J. Biol. Chem.* 255:9599–9607.

21. Krisans, S. K., M. Pazirandeh, N. Rusnak, and G. M. Keller. 1986. Characterization of peroxisomal HMG-CoA reductase activity. *Fed. Proc.* 45:361.

22. Krisans, S. K., S. L. Thompson, L. A. Pena, E. Kok, and N. B. Javitt. 1985. Bile acid synthesis by rat liver peroxisomes: metabolism of 26-hydroxycholesterol to 3 β-hydroxy-5-cholenoic acid. *J. Lipid Res.* 26:1324–1332.

23. Lazarow, P. B. 1978. Rat liver peroxisomes catalyze the β-oxidation of fatty acids. *J. Biol. Chem.* 253:1522–1528.

24. Lazarow, P. B., and C. de Duve. 1973. The synthesis and turnover of rat liver peroxisomes. V. Intracellular Pathway of Catalase Synthesis. *J. Cell Biol.* 59:507–524.

25. Lazarow, P., and C. de Duve. 1976. A fatty acyl-CoA oxidizing system in rat liver peroxisomes; enhancement by clofibrate, a hypolipidemic drug. *Proc. Natl. Acad. Sci. USA.* 73:2043–2046.

26. Leighton, F., B. Poole, H. Beaufay, P. Baudhuin, J. W. Coffey, S. Fowler, and C. de Duve. 1968. The large scale separation of peroxisomes, mitochondria, and lysosomes from the livers of rats injected with Triton WR-1339. Improved isolation procedures, automated analysis, biochemical and morphological properties of fractions. *J. Cell Biol.* 37:482–513.

27. Liscum, L., R. D. Cummings, R. G. W. Anderson, G. M. De Martino, J. L. Goldstein, and M. S. Brown. 1983. 3-Hydroxy-3-methylglutaryl coenzyme A reductase: a transmembrane glycoprotein of the endoplasmic reticulum with N-linked "high-mannose" oligosaccharides. *Proc. Natl. Acad. Sci. USA.* 80:7165–7169.

28. Liscum, L., J. Finer-Moore, R. M. Stroud, K. L. Luskey, M. S. Brown, and J. L. Goldstein. 1985. Domain structure of 3-hydroxy-3-methylglutaryl coenzyme A reductase, a glycoprotein of the endoplasmic reticulum. *J. Biol. Chem.* 260:522–530.

28a. Lowry, O. H., N. Rosebrough, A. Farr, and R. Randall. 1951. Protein measurement with the folin-phenol reagent. *J. Biol. Chem.* 193:265–275.

29. Mannaerts, G. P., L. J. Debeer, J. Thomas, and P. J. Deschepper. 1979. Mitochondrial and peroxisomal fatty acid oxidation in liver homogenates and isolated hepatocytes from control and clofibrate treated rats. *J. Biol. Chem.* 254:4585–4595.

30. Mitropoulos, K. A., and S. Venkatesan. 1977. The influence of cholesterol on the activity, on the isothermic kinetics and on the temperature-induced kinetics of 3-hydroxy-3-methylglutaryl coenzyme A reductase. *Biochim. Biophys. Acta.* 489:126–142.

31. Philipp, B. W., and D. J. Shapiro. 1979. Improved methods for the assay and activation of 3-hydroxy-3-methylglutaryl coenzyme A reductase. *J. Lipid Res.* 20:588–593.

32. Posthuma, G., J. W. Slot, and H. J. Geuze. 1984. Immunocytochemical assays of amylase and chymotrypsinogen in rat pancreas secretory granules. *J. Histochem. Cytochem.* 32:1028–1034.

33. Rodwell, V. W., J. L. Nordstrom, and J. J. Mitschelsen. 1976. Regulation of HMG CoA reductase. *Adv. Lipid Res.* 14:1–74.

34. Saucier, S. E., and A. A. Kandutsch. 1979. Inactive 3-hydroxy-3-methylglutaryl coenzyme A reductase in broken cell preparations of various mammalian tissues and cell cultures. *Biochim. Biophys. Acta.* 572:541–556.

35. Shapiro, D. J., J. L. Nordstrom, J. J. Mitschelen, V. W. Rodwell, and R. T. Schimke. 1974. Micro Assay for 3-hydroxy-3-methylglutaryl CoA reductase in rat liver and L-cell fibroblasts. *Biochim. Biophys. Acta.* 370:369–377.

36. Singer, S. J., K. T. Tokuyasa, A. H. Dutton, and W. T. Chen. 1982. *In* Electron Microscopy in Biology. Vol. 2. J. D. Griffith, editor. Academic Press, Inc., New York. 55–106.

37. Tanaka, R. D., P. A. Edwards, S. F. Lan, E. V. Knoppel, and A. L. Fogelman. 1982. The effect of cholestyramine and mevinolin on the diurnal cycle of rat hepatic 3-hydroxy-3-methylglutaryl coenzyme A reductase. *J. Lipid Res.* 23:1026–1031.

38. Tokuyasu, K. T. 1973. A technique for ultracryotomy of cell suspensions and tissues. *J. Cell Biol.* 57:551–565.

39. Weibel, E. R., W. Staubli, H. R. Gnage, and S. A. Hess. 1969. Correlated morphometric and biochemical studies on the liver cell. I. Morphometric model, sterologic methods, and normal morphometric data for rat liver. *J. Cell Biol.* 42:68–91.

40. Yonentani, T. 1967. Cytochrome oxidase: beef heart. *Methods Enzymol.* 10:332–335.

41. Young, N. L. 1979. Coping with substrate cleavage in the HMG-CoA reductase assay. *J. Lipid Res.* 20:1049.

42. Young, N. L., and B. Berger. 1980. Assay of S-3-hydroxy-3-methylglutaryl CoA reductase. *Methods Enzymol.* 71:498–593.

43. Young, N. L., C. D. Saudek, S. A. Crawford, and S. L. Zuckerbrod. 1982. Recovery and activation of hydroxymethylglutaryl coenzyme A reductase from rat small intestine. *J. Lipid Res.* 23:257–265.